

## Recording Intramolecular Mechanics during the Manipulation of a Large Molecule

Francesca Moresco,<sup>1</sup> Gerhard Meyer,<sup>1,2</sup> Karl-Heinz Rieder,<sup>1</sup> Hao Tang,<sup>3</sup> André Gourdon,<sup>3</sup> and Christian Joachim<sup>3</sup>

<sup>1</sup>*Institut für Experimentalphysik, Freie Universität Berlin, Arnimallee 14, D-14195 Berlin, Germany*

<sup>2</sup>*Paul Drude Institut für Festkörperelektronik, Hausvogteiplatz 5-7, D-10117 Berlin, Germany*

<sup>3</sup>*CEMES-CNRS, 29 rue J. Marvig, P.O. Box 4347, F-31055 Toulouse Cedex, France*

(Received 6 April 2001; published 2 August 2001)

The technique of single atom manipulation by means of the scanning tunneling microscope (STM) applies to the controlled displacement of large molecules. By a combined experimental and theoretical work, we show that in a constant height mode of manipulation the STM current intensity carries detailed information on the internal mechanics of the molecule when guided by the STM tip. Controlling and time following the intramolecular behavior of a large molecule on a surface is the first step towards the design of molecular tunnel-wired nanorobots.

DOI: 10.1103/PhysRevLett.87.088302

PACS numbers: 82.37.Gk, 07.79.Cz, 85.65.+h

During a spontaneous diffusion process on a surface, a large molecule adapts to the atomic landscape by means of intramolecular deformations. At a given temperature, these conformational changes permit the molecule to pass over the surface potential barriers encountered during its random motion. When now the molecule is forced by the tip apex of a scanning tunneling microscope (STM) [1] to overcome these barriers, the corresponding conformational changes lead to a shift of the energy position of the tunnel channels provided by the molecule [2] or to a change of its electronic coupling with the surface [3]. It was recently demonstrated that by means of the low temperature STM and in ultrahigh vacuum (UHV) it is possible to manipulate single atoms and small molecules [4,5]. The recording of the STM feedback loop during a manipulation sequence characterizes the semiclassical motion of the adsorbates under the tip apex, allowing one to distinguish between different manipulation modes [6,7]. Furthermore, the time-dependent tunneling current  $I(x(t))$  through the molecule is a direct measure of its detailed intramolecular conformational change along the manipulation path (Fig. 1a).

In this Letter, we show that the lateral manipulation techniques can be applied to investigate the intramolecular mechanics of large molecules. Our aim is to induce motion and deformation of a part of a molecule on a surface in a controlled manner and to monitor in real time the resulting motion of this part. This represents the first step toward the realization of a wired molecular robot, where a physical link between the molecule and the STM tip apex can be established by their direct electronic interaction. The electronic wiring effect is prolonged inside the molecule by a molecular wire group interconnecting the moving part to the tip apex.

To record  $I(x)$ , we exploited the high stability and the low noise level of a low temperature STM (UHV-LT-STM) [8]. We used Cu-tetra-3,5 *di-ter-butyl-phenyl porphyrin* (TBPP) molecules equipped with four legs (Fig. 1) as prototypes. In a constant current mode of operation and at room temperature, molecular mechanics calculations [6,9] show that the STM manipulation of a TBPP induces a pe-

culiar alternate movement of the front leg while the tip interacts with the molecule by pushing on the rear legs. The next step is to experimentally record and interpret in real time these intramolecular motions. TBPP molecules were sublimated at minute quantities on a Cu(100) surface. A detailed comparison of the registry of the molecules with the surface lattice indicates that the TBPP are physisorbed in only one orientation. In the STM image, a TBPP shows four bright lobes with some lateral residual echoes (Fig. 1c). Calculations of the full STM image of a TBPP on Cu(100), performed by the elastic scattering quantum chemistry (ESQC) technique [10], show that each lobe corresponds to a leg oriented not exactly perpendicular to the surface, with  $\Theta_1 = 79^\circ$ ,  $\Theta_2 = 67^\circ$ ,  $\Theta_3 = 75^\circ$ , and  $\Theta_4 = 83^\circ$  (Fig. 1).

Constant height scans recorded at a temperature  $T = 12$  K over one TBPP at different altitudes are shown in Fig. 2. They were measured by passing with the tip over the center of the molecule at tip-surface distances between 12 and 9 Å. Depending on the direction of approach and on the path of the tip across the molecule, the tip apex interacts with the legs already at a tip-surface distance between 12 and 13 Å, demonstrating that there is a large range of tip apex altitudes where the molecule interacts with the tip apex without being manipulated. Sudden variations in the signal can be observed at low tip-surface distances (9.3 and 8.9 Å) and are due to the strong attractive interaction between leg and tip, which gives rise to mechanical instabilities.

Our STM manipulations were performed at  $T = 12$  K in a constant height mode [7] for tip apex distances below the scanning conditions of Fig. 2, correcting during a first scan any inclination of the surface. In the more conventional constant current mode of manipulation, the tip apex distance to the surface increases as the tip approaches the molecule, minimizing the mechanical interactions between tip apex and molecule. In contrast, a constant height mode reinforces the tip apex to molecule interaction and provides the molecule with enough intramolecular deformations to overcome the surface barriers.

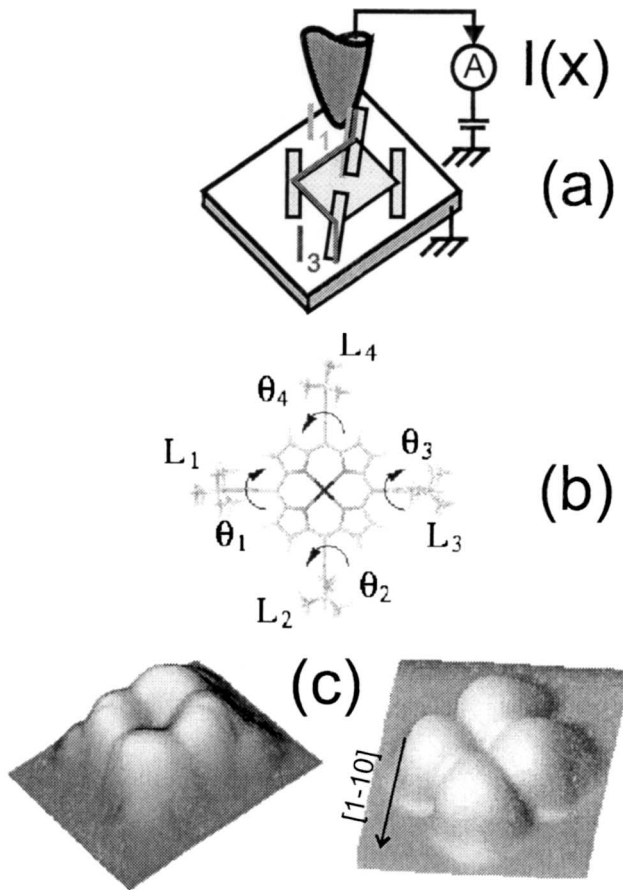


FIG. 1. (a) Schematic representation of the manipulation of a TBPP molecule. The time-dependent STM total current intensity  $I(x(t))$  recorded during the manipulation results from the superposition of the tunnel paths introduced by the four legs and carries information about the semiclassical motion and deformations of each leg through the central porphyrin ring.  $I(x(t))$  is experimentally measured versus the time-dependent displacement  $x(t)$  made by the tip on the surface during the manipulation and is therefore indicated in the text as  $I(x)$ . (b) Nomenclature assigned to legs and angles. Rotation axes are defined relative to  $90^\circ$  for a leg perpendicular to the surface. (c) Experimental STM image (left) of a TBPP adsorbed on Cu(100) and corresponding calculated image (right) with the ESQC technique (tunneling current  $I = 2$  nA and sample bias voltage  $V = 200$  mV).

In order to manipulate a TBPP and among the different possible directions by approaching the molecule with the tip apex, we used a pushing mode performed on a single leg (Fig. 3). The exact path followed by the tip is shown in the inset of Fig. 3a. The experimental and calculated  $I(x)$  of a manipulation sequence presented in Fig. 3 reflects the Cu(100) lattice periodicity. However, details in each period do not resemble the regular sawtooth  $I(x)$  signals recorded during STM manipulations of atoms and diatomic molecules [11,12]. Zoomed parts of the Fig. 3 signals are presented in Fig. 4. Manipulations and  $I(x)$  curves recorded in the other Cu(100) directions deliver also a periodic  $I(x)$  but with a different specific intra-period signature for each direction. As one can see in

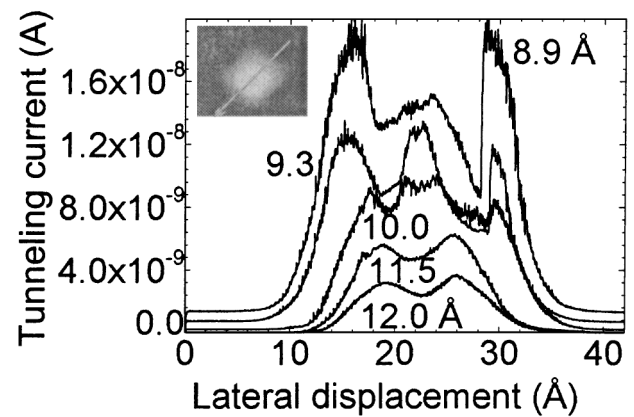


FIG. 2. Constant height  $I(x)$  tunneling current intensity recorded over a TBPP molecule at different altitudes. The tip apex approaches over the center of the molecule, at a bias voltage  $V = -50$  mV. The tip-surface distance,  $z$ , is defined by the center-to-center distance between surface and tip atoms at the electrical point contact. The experimental tip-surface separation at the electrical point contact corresponds to  $z = 4$  Å. The exact path of the tip is shown in the inset. The tip-molecule distance is kept large enough to avoid the manipulation of the molecule.

Fig. 3, the experimental starting sequence is not fully reproduced by the theory. Such initial oscillation critically depends on the exact initial position of the tip apex on the leg and has been experimentally observed to change from manipulation to manipulation.

To extract from  $I(x)$  the intramolecular mechanics occurring during a manipulation sequence, we performed detailed molecular mechanics plus STM-ESQC current calculations of the process. For reference, we considered first a fully rigid molecule manipulated along the Cu(100) surface. It results in a very regular  $I(x)$  with no submodulation inside each period (Fig. 4b, dashed line), corresponding to the STM pushing of a large rigid nanoscale object on a periodic surface. Performing now our calculations with a nonrigid molecule leads to an  $I(x)$  very close to the experimental one (Figs. 3b and 4b).

When the molecule is manipulated via the leg labeled  $L_1$  (Fig. 1), we have calculated that each  $\Theta_i$  reaches a steady averaged rotation angle of  $\Theta_1 = 59^\circ$ ,  $\Theta_2 = 66^\circ$ ,  $\Theta_3 = 64^\circ$ , and  $\Theta_4 = 71^\circ$ . Corresponding to the recorded  $I(x)$ , the variations around these average values are, respectively,  $\Delta\Theta_1 = 1^\circ$ ,  $\Delta\Theta_2 = 0.4^\circ$ ,  $\Delta\Theta_3 = 0.9^\circ$ , and  $\Delta\Theta_4 = 0.3^\circ$ . Furthermore, the center of mass of the molecule for lateral motion is restricted by the Cu(100) surface atomic corrugation and by the attraction exerted on  $L_4$  by the tip apex which precludes  $L_3$  to be a pivotal point during a manipulation sequence. The easy rotational axis of  $\Theta_2$  and  $\Theta_4$  is parallel to the manipulation direction leading to a small  $\Delta\Theta$  for those legs.

To extract, for example, the sequence of deformation corresponding to the legs  $L_1$  and  $L_3$  during manipulation, we have plotted in Fig. 4c the calculated variations of  $\Theta_1(x)$  and  $\Theta_3(x)$ .  $L_1$  is the main contributor to  $I(x)$  because of its direct interactions with the tip apex. We found

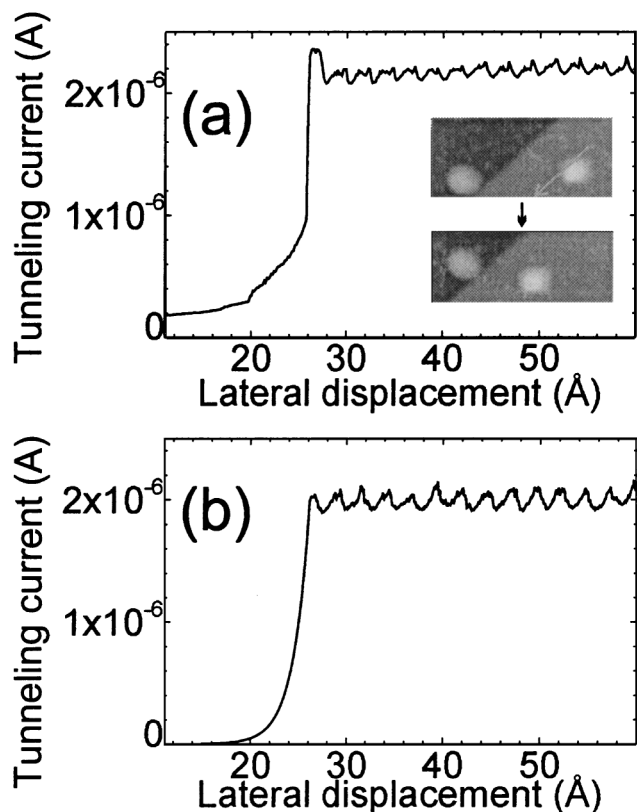


FIG. 3. (a) Experimental  $I(x)$  curve recorded over a TBPP molecule along the  $[1-10]$  direction during lateral manipulation performed on a single leg at a tip-surface distance of  $9.6 \text{ \AA}$  and at a bias voltage  $V = -50 \text{ mV}$ . In the inset STM images recorded before and after the manipulation are shown. The arrow indicates the exact path of the tip during the process. (b) Calculated current signal corresponding to the manipulation signal in (a).

that, after an initial sequence of attraction and repulsion between  $L_1$  and the tip apex to reach the average angle  $\Theta_1 = 59^\circ$  (not presented), the first  $I(x)$  little maximum  $M_1$  in each  $I(x)$  period corresponds to a repulsive interaction between the front  $\text{CH}_3$  group of  $L_1$  and the Cu surface atoms, while this leg is pushed by the tip apex. It results in a small  $\Theta_1$  increase ( $A_1$ ), until the front  $\text{CH}_3$  passes over the Cu atom. Then, both rear and front  $\text{CH}_3$  groups reach a stable position on Cu(100), where the Cu atom lies between the two  $\text{CH}_3$  groups. This corresponds to a minimum ( $A_2$ ) in  $\Theta_1$ . The situation favors an increase of the electronic interaction between the central part of  $L_1$  and the surface, inducing the large ( $M_2$ ) peak in  $I(x)$ . Then,  $\Theta_1$  increases ( $A_1$ ) until the  $\text{CH}_3$  groups are both in repulsive interaction with the surface. This lowers the electronic interaction between leg and surface leading to a sharp ( $M_3$ ) minimum per period. The sequence ( $M_1, M_2, M_3$ ) reproduces itself from period to period. However, the current signal shows fluctuations because the local mechanics of the  $\text{CH}_3$  groups just described can be modified (especially  $A_1$ ) by a lateral rotation of the leg in favor of the third  $L_1$  bottom  $\text{CH}_3$  group.

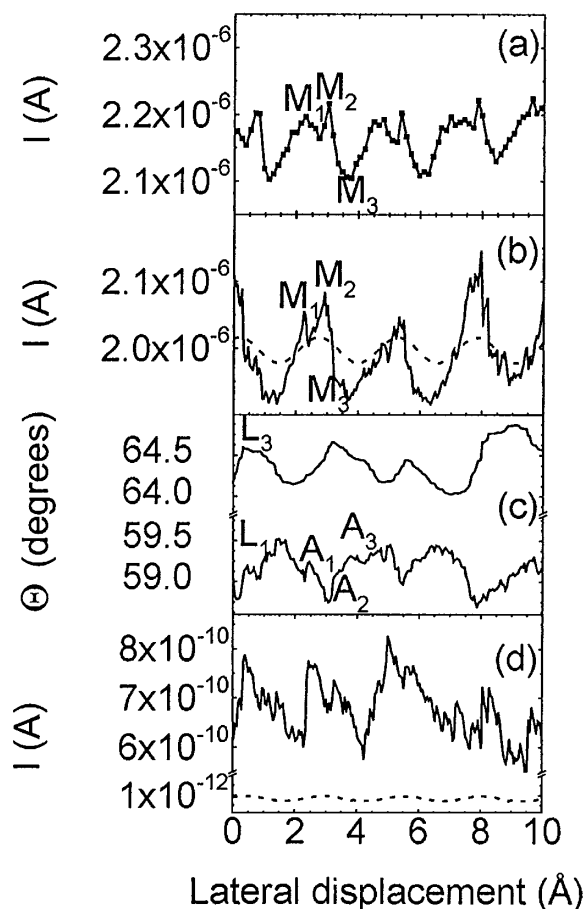


FIG. 4. Details of the experimental and calculated manipulation signal  $I(x)$ . (a) Experimental  $I(x)$  during a manipulation sequence taken over four periods. The  $M_1$  and  $M_2$  maxima and the  $M_3$  minimum are indicated. (b) Calculated  $I(x)$  at a tip apex to surface distance of  $9.5 \text{ \AA}$  associated with the experimental  $I(x)$  in (a). The dashed line shows the result of the same calculation for a rigid TBPP.  $M_1, M_2,$  and  $M_3$  have been indicated too. (c) Characteristic conformations ( $\Theta_i$ ) for  $L_1$  and  $L_3$  corresponding to  $I(x)$  in (b).  $A_1, A_2,$  and  $A_3$  refer to the leg  $L_1$  and are discussed in the text. The variations of  $\Theta_3$  are more regular due to the absence of a direct tip apex interaction. We found no evidence of altitude variation of the porphyrin relative to the surface during a manipulation sequence. (d)  $I_3(x)$  component of  $I(x)$  corresponding to the  $L_3$  deformation extracted from the  $I(x)$  total signal (b). The dashed line shows the result of the same calculations for a rigid TBPP, choosing for  $\Theta_3$  its equilibrium value. In the ESQC calculations, 576 atoms were taken into account in the STM junction, 247 for the pyramidal tip apex, 156 for the surface, and 173 for the TBPP, taking into account a total of 819 molecular orbitals.

Such a very fine analysis of the TBPP intramolecular deformation during a manipulation sequence demonstrates that detailed “on line” information on the internal mechanics of a molecule can be extracted from  $I(x)$  during many periods. To go further, we consider now how  $I(x)$  results from the superposition of four tunnel paths, one per leg, and how the deformation of  $L_3$  contributes to  $I(x)$ . This leg is particularly interesting to follow up because it offers the larger  $\Delta\Theta$  among  $\Theta_2, \Theta_3,$  and  $\Theta_4$  and because it is

not in direct interaction with the tip apex. The central porphyrin ring electronically wires  $L_3$  to the tip apex reporting about the  $L_3$  motion during a manipulation sequence.

The branching node for this superposition is the sigma bond attaching  $L_1$  to the porphyrin ring. Per section, this ring plays the role of an intramolecular wire interconnecting the  $L_2$ ,  $L_3$ , and  $L_4$  tunnel paths to the  $L_1$  node. Applying the superposition rule for a single intramolecular tunnel node [13], the tunnel paths are separable leg by leg. We have calculated  $I(x)$  by suppressing in ESQC, respectively, all the molecular orbitals responsible for a given leg tunnel path while keeping unchanged the full TBPP mechanics. We confirm that while  $L_1$  is the main contributor to  $I(x)$  due to its close proximity to the tip apex,  $L_2$ ,  $L_3$ , and  $L_4$  contribute too. Their respective contributions are  $\Delta I_2 = 70$  pA,  $\Delta I_3 = 200$  pA, and  $\Delta I_4 = 130$  pA. The large  $\Delta\Theta$  of  $L_3$  compensates for its large separation to the tip apex compared to  $L_4$ . The  $I_3(x)$  component of  $I(x)$  associated with the  $L_3$  motion we are interested in here is presented in Fig. 4d. It is modulated by the same variations as  $\Theta_3$ , but free from direct repulsive tip apex interaction. The maxima in  $\Theta_3$  correspond to manipulation sequences where the interactions between the  $L_3$  end atoms and the surface are large, leading to maxima in  $I_3(x)$ . With a rigidified  $L_3$ ,  $I_3(x)$  has also been calculated. The resulting signal (dashed line in Fig. 4d) is periodic and its intensity is 3 orders of magnitude lower than the real  $I_3(x)$ . Therefore, we conclude that  $I(x)$  is sensible to the motion of a leg positioned further away on the molecule (see Fig. 1). The molecular orbital mixing between the porphyrin and  $L_3$  is very sensible to small  $L_3$  conformational changes which modify the transparency of the “ $L_3$ -porphyrin-tip apex” tunnel path during a manipulation sequence. However, the  $I_3(x)$  contribution to  $I(x)$  is quite small because of the low transparency of this path. Substituting the porphyrin by a better molecular wire [14] will improve this tunneling wiring effect of a distant-to-the-tip-apex leg and will allow one to experimentally record a much more intense signal.

In conclusion, we have demonstrated how the intramolecular mechanics of complex molecules can be recorded during a manipulation sequence performed by

UHV-LT-STM. The detailed motion of the intramolecular moving parts of the molecule are extracted from the current signal measured along the manipulation path. The manipulation of a molecule equipped with wheels (instead of legs) or arms and constituted of a molecular wire as central body (to interconnect the moving parts of the molecule to the tip apex) is a conceivable next step towards the design of molecular wired nanorobots.

Partial funding was assured by the European Union programs TMR (“Atomic/Molecular Manipulation” project) and IST-FET (“Bottom-Up Nanomachines” project) and by the Deutsche Forschungsgemeinschaft (Project No. RI 472/3-2). We thank IBM for a SUR award which made available a large SP/6000 machine for STM calculations.

- 
- [1] R. Wiesendanger, *Scanning Probe Microscopy and Spectroscopy* (Cambridge University Press, Cambridge, 1994).
  - [2] C. Joachim, J. Gimzewski, R. R. Schlittler, and C. Chavy, *Phys. Rev. Lett.* **74**, 2102 (1995).
  - [3] F. Moresco, G. Meyer, K.-H. Rieder, H. Tang, A. Gourdon, and C. Joachim, *Phys. Rev. Lett.* **86**, 672 (2001).
  - [4] J. A. Stroscio and D. M. Eigler, *Science* **254**, 1326 (1991).
  - [5] P. Avouris, *Acc. Chem. Res.* **28**, 95 (1995).
  - [6] T. A. Jung, R. R. Schlittler, J. K. Gimzewski, H. Tang, and C. Joachim, *Science* **271**, 181 (1996).
  - [7] F. Moresco, G. Meyer, K.-H. Rieder, H. Tang, A. Gourdon, and C. Joachim, *Appl. Phys. Lett.* **78**, 306 (2001).
  - [8] G. Meyer, *Rev. Sci. Instrum.* **67**, 2960 (1996).
  - [9] J. K. Gimzewski and C. Joachim, *Science* **283**, 1683 (1999).
  - [10] P. Sautet and C. Joachim, *Chem. Phys. Lett.* **185**, 23 (1991).
  - [11] L. Bartels, G. Meyer, and K.-H. Rieder, *Phys. Rev. Lett.* **79**, 697 (1997).
  - [12] G. Meyer, L. Bartels, S. Zöphel, E. Henze, and K.-H. Rieder, *Phys. Rev. Lett.* **78**, 1512 (1997).
  - [13] M. Magoga and C. Joachim, *Phys. Rev. B* **59**, 16011 (1999).
  - [14] C. Joachim, J. K. Gimzewski, and A. Aviram, *Nature (London)* **408**, 541 (2000).